PROPOSAL OF METHODOLOGY FOR OBTAINING THE RESPONSE OF RANDOM EXCITED STRUCTURES

Casimiro José Gabriel
Diretoria de Engenharia Naval
20@den.mar.mil.br

Jules Ghislain Slama
Programa de Engenharia Mecânica, COPPE, Universidade Federal do Rio de Janeiro
jules@rionet.com.br

Abstract. *The work presents an experimental approach applied to problem's resolution based on punctually excited structures by an ergodic stationary randon force joining vibration, noise generation and transmission in aeronautics and naval vehycles. It permits to predict the structure response as displacement, velocity or acceleration, as well as internal forces, power flow in each structural element and power transmitted by means of elements coupling.*

Keywords*. coherent vibratory fields, ergodic stationary randon fields, experimental methodologies*

1. Introduction

The methodology presented, named "Energetic Modal Interpolation Methodology" (MIME), is an alternative approach to the metrological treatment of problems regarding vibrating structures excited by a punctually ergodic stationary random force. It is essentially experimental, and it is based on the concepts of field projection in coherent references, which main application is in aeronautical, astronautics and naval vehicles. It is also expected to be integrated to sound problems interacting vibrating structures and the surrounding fluid environment.

The application of MIME demands the knowledge of the eigenfunctions associated with the vibration model, that can be obtained by analytical or numeric methods, such as the Finite Element Method (FEM), for instance, and the development of an algorithm to process experimental data, applying the Minimum Square Principle. Thus, for each structural component, it will be possible to obtain displacement representations (or velocity and acceleration), internal forces and power flows regarding each force.

The power flow represents the rate of work carried out or the rate of energy supplied to a system. The vibrating power transmitted through structural components is dissipated by damping, transformed in heat and irradiated as sound energy, causing, sometimes, undesirable levels of vibration and noise. Therefore, it is essential to know vibrating power propagation mechanisms and energy transmission paths to the analysis, diagnosis and control.

The analysis will be limited to simple geometry structures.

2. Theoretical basis

The response $u(x,t)$ of a vibrating structure submitted to a punctual excitation $F(t)$ applied in a point x_0 consists of the resolution of an equation of the following type:

$$\left\{L(x)+M(x)\frac{\partial^2}{\partial t^2}\right\}u(x,t)=F(t)\delta(x-x_0) \tag{1}$$

where $u(x,t)$ is displacement, $x=(x_1,x_2,x_3)$ the position vector, $L(x)$ a self-adjoint differential operator that includes derivatives in relation to the space co-ordinates x_1 and x_2, t is time and $M(x)$ mass distribution. By the Expansion Theorem, the solution may be written in an infinite series form, as an overlap of normal modes $U_r(x)$ named eigenfunctions (AF), multiplied by the corresponding generalised co-ordinate functions $\eta_r(t)$:

$$u(x,t)=\sum_{r=1}^{\infty}U_r(x)\eta_r(t) \tag{2}$$

A second way to express $u(x,t)$ in any point of domain $D_{(x)}$ is through the integral equation:

$$u(x,t)=\int\int_{D_{(x)}} G(x,x';t,t_i)F(t_i)\delta(x'-x_0)d\,D(x')\,d\,t_i \tag{3}$$

where $G(x, x_0; t, t_i)$ is the Generalised Green Function. When applying Fourier Transform to (3), it is obtained:

$$u(x,f) = G(x, x_0, f)F(f) \tag{4}$$

where f is the frequency. Thus, it can be concluded that the whole field is coherent, since the Ordinary Coherence Function between the displacement and the excitation $(\Gamma^2_{uF}(f))$ is equal to 1, $\forall$f.

This result justifies the procedure adopted in MIME: since the whole field is coherent, the response can be obtained in the frequency domain by means of the procedure known as "field decomposition in an ortogonal reference *r(t)*", or as "field projection on *r(t)* ", which is useful for harmonic or stationary random excitation problems, and *r(t)* should be chosen as a function with no-void coherence with F(*t*). If S_{ru} is the crossed spectrum between the reference and the response, the Crossed Spectrum Function of a displacement in two points x_1 and x_2, $S_{uu}(x_1, x_2, f)$, can be written according to the field projection on $r(t)$ with the aid of a Frequency Response Function $H(x,f)$, where $H(x,f)$ is:

$$H(x,f) = \frac{S_{ru}(x,f)}{S_{rr}(f)} \tag{5}$$

$$S_{uu}(x_1, x_2, f) = H^*(x_1, f)H(x_2, f)S_{rr}(f) = \frac{S_{ur}(x_1, f)S_{ru}(x_2, f)}{S_{rr}(f)} \tag{6}$$

Equation (6) shows the spectrum divisibility, a feature only applied for sinusoidal or coherent fields. In vibrating fields, $H(x,f)$ obeys the Wave Equation, because it is proportional to the field crossed spectrum with a reference, and the field Crossed Spectrum Function verifies the Wave Equation for one of the variables. Based on this feature, the reference Crossed Spectrum Function can be extrapolated or interpolated. Similarly, in the case of acoustic fields, $H(x,f)$ obeys Helmholtz Equation, and the reference Crossed Spectrum Function should also be known on a surface around the sources. In this case, there is an equivalence among coherent stationary random fields and sinusoidal fields.

Thus, $r(t)$ might be chosen as a point field value, or as an electric tension value, or as the vibration velocity of a space structural component, provided that tension and vibration velocity are associated with the field determination. If choice relapses into the signal of excitation itself, the use of experimental parameters $S_{FF}(f)$ and $H(x,f)$ supplied by analysers is possible, and Wave Equation in the frequency domain can be transformed into:

$$\left\{L(x) - (2\pi f)^2 M(x)\right\} S_{Fu}(x,f) = S_{FF}(f)\delta(x - x_0) \tag{7}$$

where S_{Fu} is the Crossed Spectrum Function between excitation and displacement, which solution, specified in the Expansion Theorem is:

$$S_{Fu}(x,f) = \sum_r^{\infty} \alpha_r(f) U_r(x) \tag{8}$$

To obtain the coefficients α_r it is not necessary to know the Generalized Coordinated Functions $\eta_r(t)$: they have to be associated to the minimization of the error that occurs when the series terms number is limited. The procedure consists of measuring $S_{Fu}(x,f)$ in x_j points along the structural element, and applying the following relation k times, where k is the number of the finite series terms:

$$\sum_j S_{Fu}(x_j, f)U_k^*(x_j) - \sum_i \alpha_i(f) \sum_j \left\{U_i(x_j)U_k^*(x_j)\right\} = 0 \tag{9}$$

The finite series will be named, from now on, "interpolated function "(FI). Coefficients α_r are determined by the resolution of a matricial equation of type $X = A^{-1}Y$.

The displacement Crossed Spectrum Function measured in two points x_1 and x_2 will be:

$$S_{uu}(x_1, x_2, f) = \frac{1}{S_{FF}(f)} \sum_r \sum_s \alpha_r^*(f)\alpha_s(f)U_r^*(x_1)U_s(x_2) \tag{10}$$

Since the other magnitudes, such as internal forces acting in a structural element, and power flows are determined by successive derivatives in relation to the position of an analytical expression close to the linear displacement function, they are calculated by means of the space derivatives of the Crossed Spectrum Function between two points:

$$S\frac{\partial^n u}{\partial x^n}\frac{\partial^m u}{\partial x^m}(x_1, x_2, f) = \frac{S\frac{\partial^n u}{\partial x^n}{}_F(x_1, f)\, S_F\frac{\partial^m u}{\partial x^m}(x_2, f)}{S_{FF}(f)} \tag{11}$$

3. Tests, spatial sampling and execution methodology

Tests consisted in exciting a two-beamed structure in relation to a right angle (in "L"shape) by a punctual force with a wide spectrum random variation (white noise). Frequency range was chosen between 0 and 3 kHz. The structure was suspended through nylon threads, so as to set free/free boundary conditions.

Beams were identical and made of steel, with the following dimensions: a) length: 1 m; b) rectangular straight section, with: base = .038m; height = .0127m. Rotating inertia effects and shear deformations were not considered.

The electro-dynamic exciter acted in the free extremity of one of the beams, from now on named Beam 1. The beam directly coupled will be refered to as Beam 2. The strength was measured by a transdutor coupled to the vibrator. The signals of strength and acceleration were read by a signal analyzer that made calculations and filed the Frequency Response Function. Figure (1) shows the equipment arrangement.

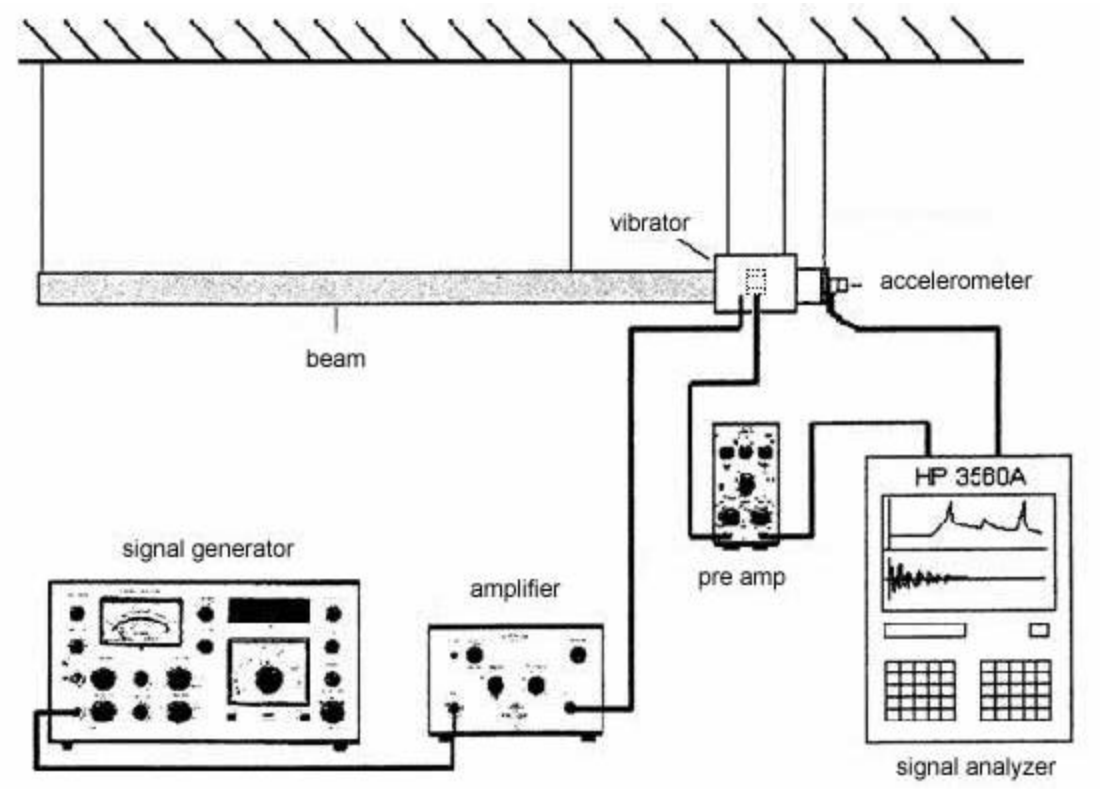

Figure (1) – Equipment arrangement.

The following tests were driven:

a) Transverse excitation, in the plan defined by beams ("parallel" excitation);

b) Transverse excitation, ortogonally to the plan defined by beams ("ortogonal" excitation);

c) Longitudinal excitation ("longitudinal" excitation)

In order to avoid the phenomenon known as "space overlap", the measured points followed a sampling rate (Δx_A) such as $(\Delta x_A) \leq l/2$, where l is the wavelength. The influence of the eigenfunctions number (NAF) and of the sampling number points (NPA) in FI were verified: this one should contain a minimum NAF equal to the immediately superior frequency resonance order. The sampling according to a minimum NPA allows to obtain solutions with small errors along each beam length. As the bending angular speed and the internal forces are associated with displacement space derivatives of orders 1, 2 and 3, it is necessary to increase NAF in FI. Thus, so that the energy contained in subsequent modes might be picked, NPA should be increased, reducing Δx_A (Gabriel, 2001). It was verified that:

(i) If NPA <NAF, space overlap occurs. The representations of $u(x,f)$ don't converge to a closed solution, and the non normalized error (MENN) as a function of the position search very high values.

(ii) If NPA ≥ NAF, the representations of $u(x,f)$ converge to a closed solution. MENN decreases as NAF and NPA increase in the representation

Considering the frequency range analysed, it was chosen to measure the response with the accelerometer at each 5 cm, in both beams, starting from extremities. As all beams had standard length equal to 1m, 21 readings were made in each one, what was enough to avoid the undesirable effect of overlapping (space aliasing).

For simulated results, The Power Spectrum of excitation was supposed constant and equal to $1\ (Newton)^2 / Hz$ throughout the whole frequency range, and damping was obtained from $\eta = 0.1/\sqrt{f}$.

4. MIME applied to beam structures - simulated results

In the "parallel" and "longitudinal" excitation cases, coupled bending and longitudinal waves were generated in both beams, and in the "ortogonal" excitation case, coupled bending and torsional waves were generated. MIME was used taking account in each beam the two displacement effects separately, and the application of k equations defined by Relationship (8) was twice used in each one.

AF were obtained through a sample with the aid of the device "ANSYS", considering, in the case of "parallel" and "longitudinal" excitations, their transverse and longitudinal components along the beams, and, in the 'ortogonal" excitation, their transverse and rotation components around the axis due to torsion effects.

To obtain AF space derivatives in a sample way, it was needed to approximate AF by a continuous function. Two approaches were tried: in the first, "spline" was used, and derivatives were calculated through the Finite Differences Method (MDF): it presented considerable errors, due to the adopted interval, equal to 5 mm, especially in the second and third order derivatives, which is the reason why they became unfeasible to power flow determination. In the second, the polinomial approach was used, and the resulting derivatives were immediately found out, being appropriate for the frequency range chosen. As a consequence, the error minimisation along each beam was also dependent on the chosen polynomial degree.

The responses obtained through MIME will be compared to the responses given by the "Closed Solution" (SF) application, presented in the Appendix, reached through the Wave Equation resolution by variable separation (always in black), having been considered two SF for each beam:

(i) "Parallel" and "longitudinal" excitations: Equations 10-1 and 10-2.

(ii) "Ortogonal"excitation: Equations 10-1 and 10-3.

where constants were determined considering the free/free condition in both extremities, excitation in Beam 1 extremity, and displacements and internal forces continuity in the joint (Gabriel, 2001). Only the results for ortogonal excitation will be showed.

4. 1 - Determination of transverse displacement (u_B), and of power due to the shearing force (P_V) and to the bending moment (P_M)

Independently from the active type of excitation, to obtain a representation of transverse displacements, as well as to obtain P_V and P_M, the best approaches for AF transverse components occurred for polynomials which degrees (g) varied between (NPN + 6) and (NPN + 8), where NPN is the number of nodal points. The degree should also necessarily be greater than 4, to prevent space derivatives of orders 1, 2 and 3 void along each beam length, or the derivative of order 3 corresponding to a linear function.

For 445Hz, corresponding to the 6^{th} vibration mode in the "ortogonal" excitation, the transverse displacement as a function of the position is represented in Fig.(2), considering FI containing the first 18 AF. Approaches used polynomial degrees g1 = NPN + 4 (green), g2 = NPN + 6 (blue) and g3 = NPN + 8 (red). The resulting representations seem to coincide visually. However, while showing the non normalised error, it is observed that the representation for g1 supplies the largest mistakes, especially in the extremities.

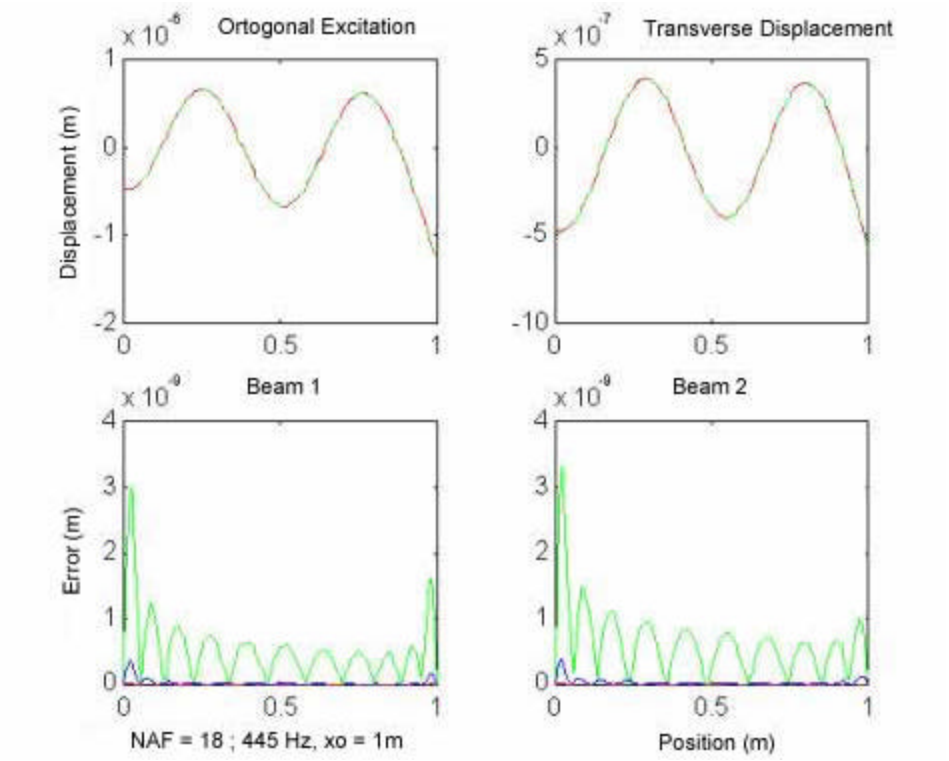

Figure 2 - SF X MIME. Transverse displacement, "ortogonal" excitation.

In Fig. (3) and (4), representations for P_V and P_M are showed. As previously said, they diverge close to the extremities for g1, where the largest mistakes are verified in transverse displacement representations (Fig. (2)).

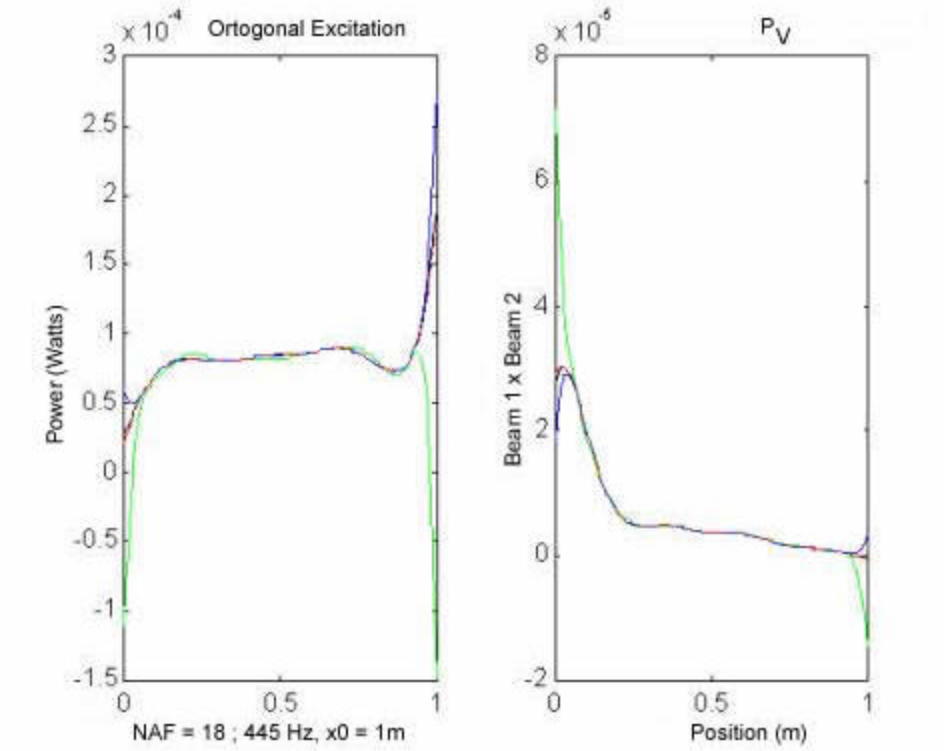

Figure 3 - SF X MIME. Determination of P_V , "ortogonal" excitation.

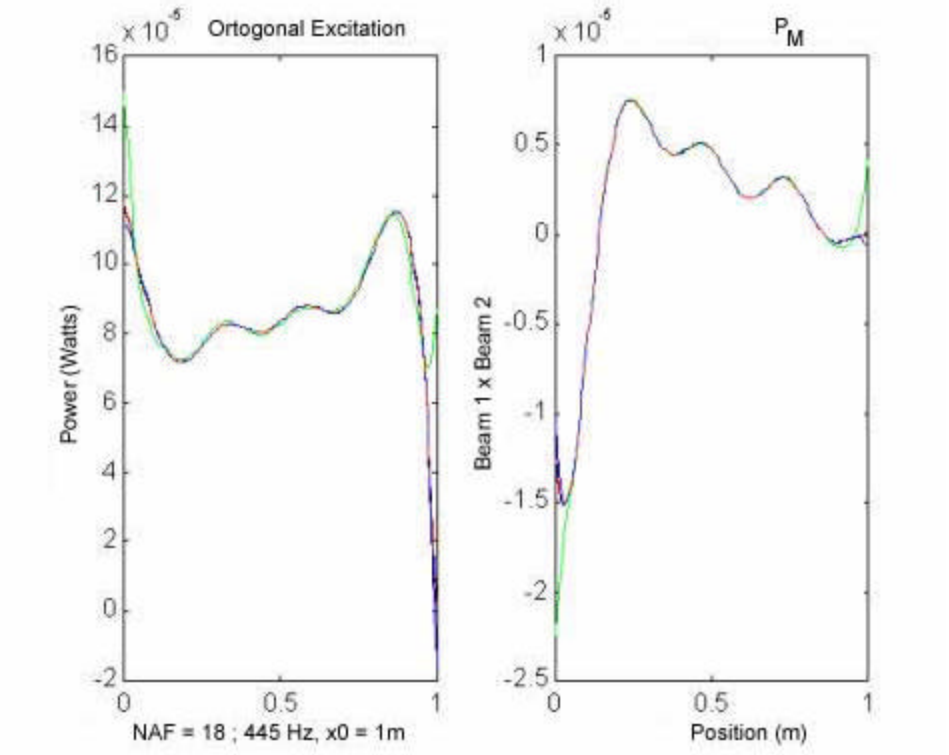

Figure (4) – Determination of P_M, "ortogonal" excitation.

Figure (5) shows P_V (superior) and P_M (inferior) transmitted in the joint, according to the frequency, in the analysis of Beam 1. Each FI used 12 AF immediately above the superior resonance frequency order. Eigenfunction transverse components were approximated by polynomials of degrees g2 = NPN + 6 (blue) and g3 = NPN + 8 (red).

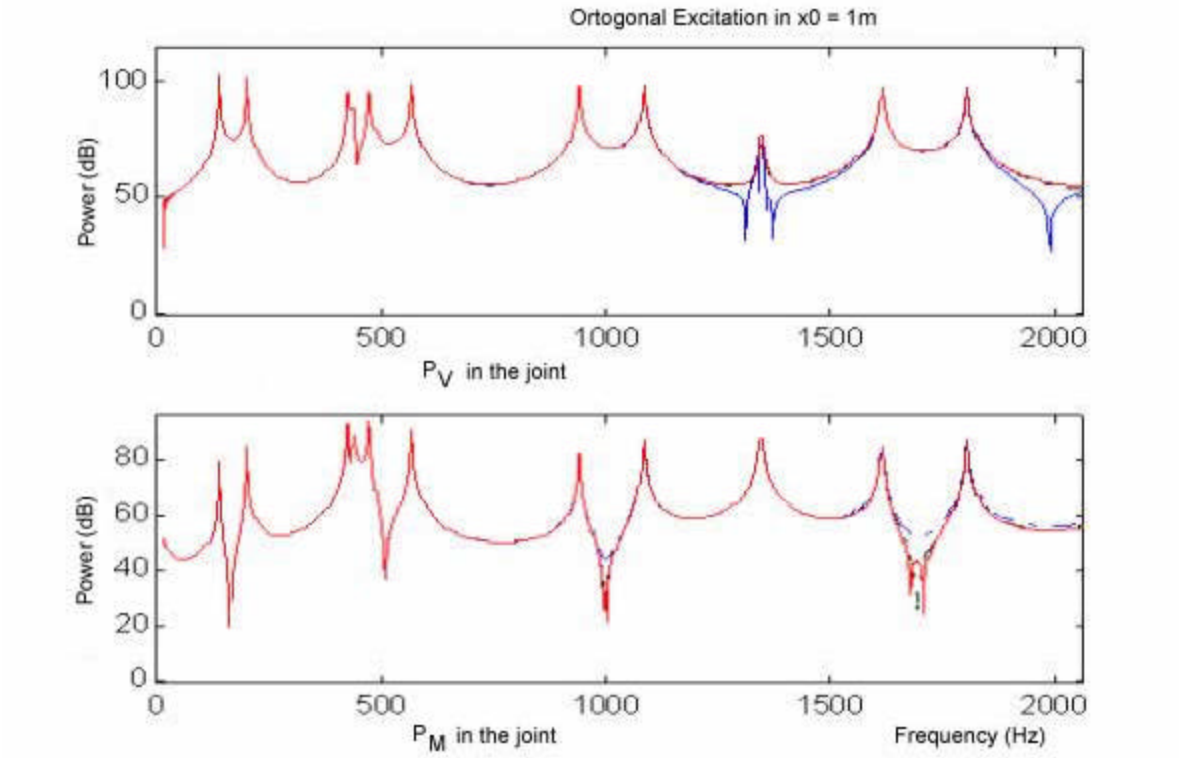

Figure 5 - SF X MIME, Beam 1, P_V (superior) and P_M (inferior) in the joint as a function of frequency.

In the three types of excitation, errors related to the determination of P_M were smaller than those related to P_V, although visually, SF and the polinomial solutions for P_V and P_M overlap in almost the whole extension of the frequency range. This seems to be probably interrelated: a) the orders of derivatives involved (1 and 2 in the case of P_M, and 3 in the case of P_V); b) the adopted sampling in AF determination; c) the approach itself: polinomial. As a direct consequence of the poor numeric properties of polynomials, the approach becomes less soft as degree increases. The representative polynomial curve tends to be distant enough from the real curve close to the extremities, what explains the existence of an empirical limit to the maximum degree in the range, equal to NPN+8. Better representations should be obtained for AF sampled from smaller intervals. In this case, "spline" AF may present a better result.

4. 2 - Determination of longitudinal displacement(u_L), torsional angular displacement (q_T), and powers due to the longitudinal force (P_L) and to the torsional moment (P_T)

Considering the torsional angular displacement and P_T, representations that use AF angular components approximated by low degree polynomials are satisfactory for frequencies up to 1 kHz, once the first mode due to torsion occurs between 1 and 1,5 kHz, since (g)>2, to avoid the torsional moment along each beam represented by a void function or a linear function. Similar observations are valid for the longitudinal displacement and P_L.

Figure (6), on the superior half, shows q_T and, on the inferior half, P_T as a function of position for 773 Hz, and polynomial representations of degrees g1 = 2 (blue), g2= 3 (red) and g3 = 4 (green).

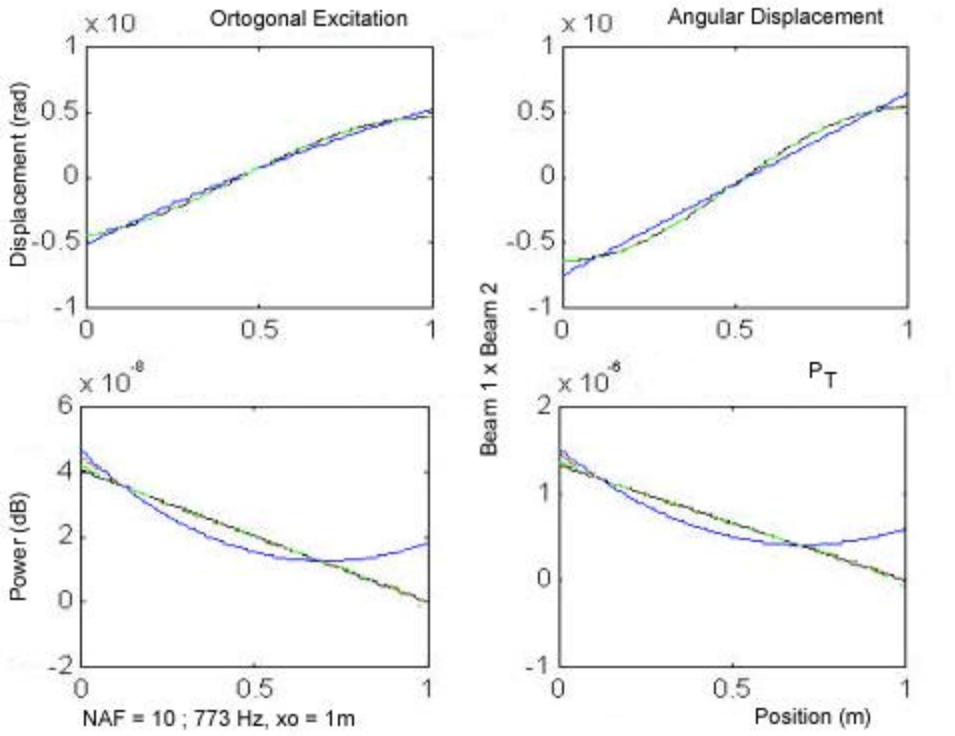

Figure 6 - SF X MIME. Determination of q_T (superior) and P_T (inferior); "ortogonal" excitation.

Figure (7) shows P_T transmitted in the joint as a frequency function, Beam 1, where FI used contained 9 (superior) and 12 (inferior) AF above the immediatelly superior resonance order. The angular displacement components of AF around the torsion axes were approximated by polynomials of degrees g2 = 3 (blue) and g3 = 4 (red).

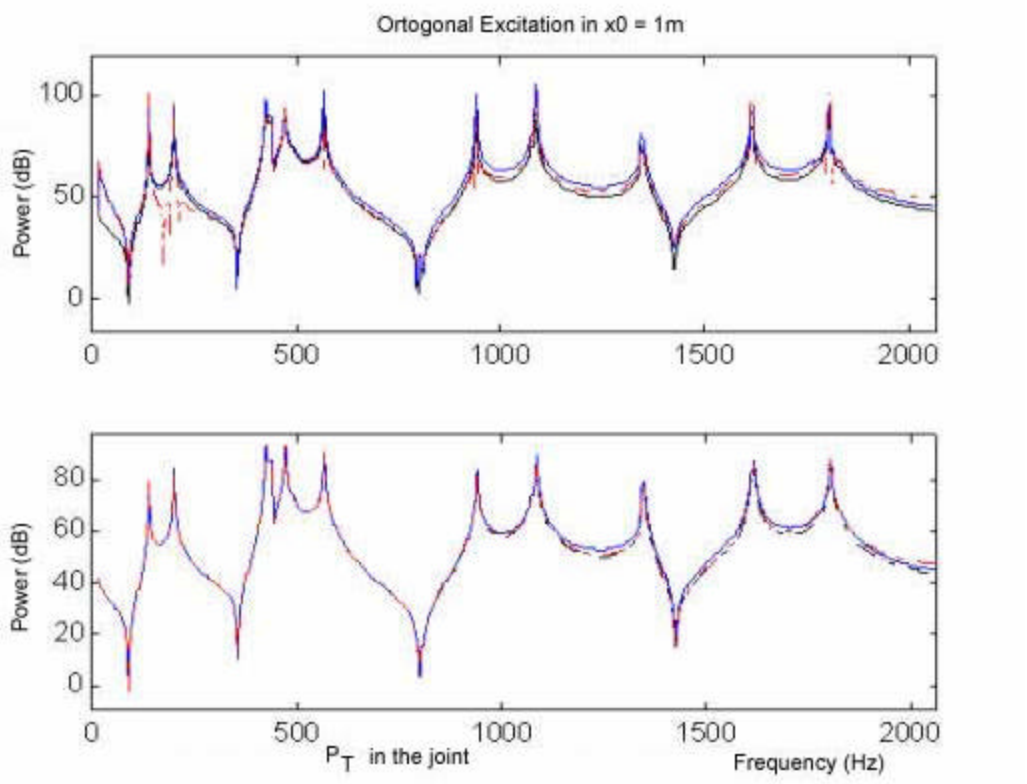

Figure 7 - SF X MIME: Beam 1, P_T in the joint, as a function of frequency.

4. 3 - Total power (P_t) determination

Total power can be calculated in two different ways: first, as the sum of the individual powers due to each internal force, demanding a FI where NAF is much larger than the immediately superior resonance frequency order. Second, using the concept of dissipated power along the element:

$$P_t(x,f) = (2\pi f)\Im\{e - e'\} \tag{12}$$

where e is the total energy dissipated by the beam, and e' is the energy dissipated between the point of force application and the x coordinate point analysed. In the "ortogonal" excitation case, it is equal to:

$$e = (1/2)m\Sigma\left|v_B(x_j,f)\right|^2 + (1/2)I_P\Sigma\left|w_T(x_j,f)\right|^2 \tag{13}$$

where, v_B is the transverse velocity, w_T the torsional angular velocity, and I_P the polar moment of inertia. As v_B and w_T are obtained from time derivatives of transverse displacement and of angular torsional displacement, if FI contains NAF minimum, it already provides a good approach to total power representation. For "parallel" and "longitudinal" excitations, the same observations are still valid, but the last term of (13) should be replaced by a similar term regarding longitudinal force effect.

5. Application in coupled beams - experimental results

Representations obtained through tests were contrary to the results obtained through simulation. As NAF and NPA were increased, transverse displacement and power flow representations became more distorted in relation to their correspondents obtained through simulation, changing results. The most plausible justifications refer mainly to the experimental assembly, but also to other factors not precisely detected, that, altogether, gave raise to the presence of a corrupted signal in measurements overlapping the desired signal, which could be caused by the following factors:

(i) Equipment restriction;

(ii) Change of the system mass distribution configuration, according to the accelerometer positioning along the beam, and probable error introduction due to the contact of the accelerometer with the structure;

(iii) Energy increase caused by the contribution (contamination) of modes located outside the frequency range of interest (transmission by non resonant modes).

When a corrupted signal is present, the AF increase in the representation implies a surplus of precision in the polluted signal. The introduced mistakes suggest the following changes in the measurement procedure:

(i) Use of laser instrumentation (interferometer) or of capacity displacement transducer to avoid contact between equipment and structure;

(ii) If the suggested instrumentation is not available, than, for low frequencies, all signals may be simultaneously collected, using an accelerometer for each measurement point. Since the random signal is ergodic and stationary, the test can be theoretically made with the collection of a signal related to a measurement point. Practice demonstrated that mistakes can occur;

(iii) In case polluted signals in measurements persist, the field decomposition procedure can be tried in more than a reference, admitting the polluted signal in the exit. The approach requests the use of the Partially Spectral Analysis together with the Partial Coherence Function Theory (Gabriel, 1993).

6. MIME applied to plate structures

A simple example will be simulated involving joining between two identical steel plates, simply supported in all sides, with the following dimensions: a) major side (L_X) = 1,00 m; b) minor side (L_Y) = 0,50 m; thickness (h) = 6,35 mm. The force $F(x_0, y_0)$ acts in Plate 1, in a point of co-ordinates $x_o = 0{,}300\,m$ and $y_o = 0{,}375\,m$. Joining occurs in one of the sides, according to Fig. (8), on the left.

As a direct consequence of the boundary conditions, joining between the plates may be considered hinged, permitting the transmission of only the bending moment. The bending moments $M_2(x)$ e $M_3(x)$ distributed along the joint act in Plates 1 and 2, respectively, according to Fig. (8) on the right, which supplies a transverse view of internal forces in each plate. Thus, the response of Plate 1 corresponds to the overlap of effects due to the punctual excitation and to the distributed moment along the joint, and, the one of Plate 2, only to the distributed moment along the joint.

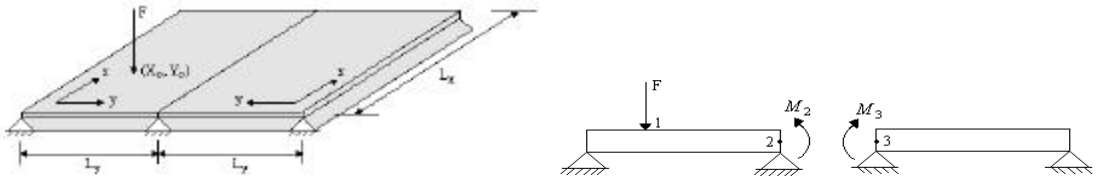

Figure 8 - System with two coupled plates: a) Left: Tri-dimensional view; b) Right: Transverse view with the acting moments along the joint.

Since the problem involves two coupled plates which geometric and stiffness parameters are identical, the existence of two vibration mode classes may be considered, corresponding, respectively, to the situations of totally uncoupled and totally blocked system, and that, together, form the coupled system, which response is the overlapping of two classes.

In the uncoupled response, the other component does not offer resistance to the movement of the component analysed. The two plates vibrate in the same mode, and they make it in phase: the joint twists, what gives to components a behavior of uncoupled structure. Associated resonance frequencies correspond to the ones of the simply supported plates in all sides.

In the blocked answer, the component of interest behaves as if it were clamped, because its movement is totally blocked by the movement of the other component. The two plates vibrate in the same mode, but they make it in opposition phase: the resultant in the joint side is void. Associated resonance frequencies correspond to the ones of the plate clamped along the joint and simply supported in the other sides.

6.1-Analytical formulation

Analytical formulation consists in relating the distributed moments to excitation sampling the joint line in constant intervals and applying the Mobility Method (Cuschieri (1996)). The amount of sampling points should reflect the frequency range of interest. The boundary conditions request the angular velocity continuity and the result from internal forces void along the joint. As plates are identical, the problem is limited to the resolution of the matrix equation

$$\{Y_{22}\}[M] = 0{,}5\,\{Y_{12}\}F \tag{14}$$

where Y_{12} is the mobility matrix that relates the angular velocity along each sampled point of the joint to the excitation, of order (NI) x (NI), where NI is the number of sampling points, $[M]$ is the matrix which components are the moments

that act in each point of the joint, and Y_{22} is the mobility matrix that relates angular velocities in each point to the moments that act in each sampled point of the joint, both of orders (NI) x 1. The expressions for the mobilities were developed and applied by Bonifácio (1998).

Once the moment along the joint is known, the power transferred along the coupling is:

$$P_M(f) = 0{,}5 \sum_{i=1}^{NI} \mathrm{Re}\left\{M(x_i,f)\, w_B^*(x_i,f)\right\} \tag{15}$$

6.2 – MIME formulation

The response obtained by means of MIME considered, in each frequency, FI with 12 AF besides the order of the immediately superior resonance frequency. Each plate was sampled through a 25 x 25 element array. For Plate 1, the processing of the algorithm in order to determine coefficients of FI joined two types of AF, one associated with the movement of a plate simply supported in the four sides (U_{r_1}) and the other associated to a plate clamped along the joint, and simply supported in the other sides (U_{r_2}) (Leissa (1993)). For Plate 2, the same algorithm only considered (U_{r_2}). Being ρ density and D the elasticity modulus for a plate:

$$Ur_1(x,y) = \mathrm{sen}(k_x x)\,\mathrm{sen}(k_y y) \tag{16}$$

$$Ur_2(x,y) = = \left\{\frac{\mathrm{sen}(k_2 y)}{\mathrm{sen}(k_2 L_y)} - \frac{\mathrm{senh}(k_1 y)}{\mathrm{senh}(k_1 L_y)}\right\}\mathrm{sen}(k_x x) \tag{17}$$

where $k_x = n\pi / L_x$, $k_y = m\pi / L_y$, $(m,n = 1, 2, 3, \ldots)$; $k_2 = \sqrt{\beta^2 - k_x^2}$; $k_1 = \sqrt{\beta^2 + k_x^2}$ e $\beta^2 = 2\pi f (\rho h/D)^{1/2}$

6.3 - Results and conclusions

Figures (9) and (10) show the transverse displacement for the first uncoupled mode (79 Hz) and the first blocked mode (110 Hz), obtained by means of MIME. The maximum difference among MIME and the analytical solution was smaller than 10^{-7} %, in the presentation of the uncoupled mode in Plate 1.

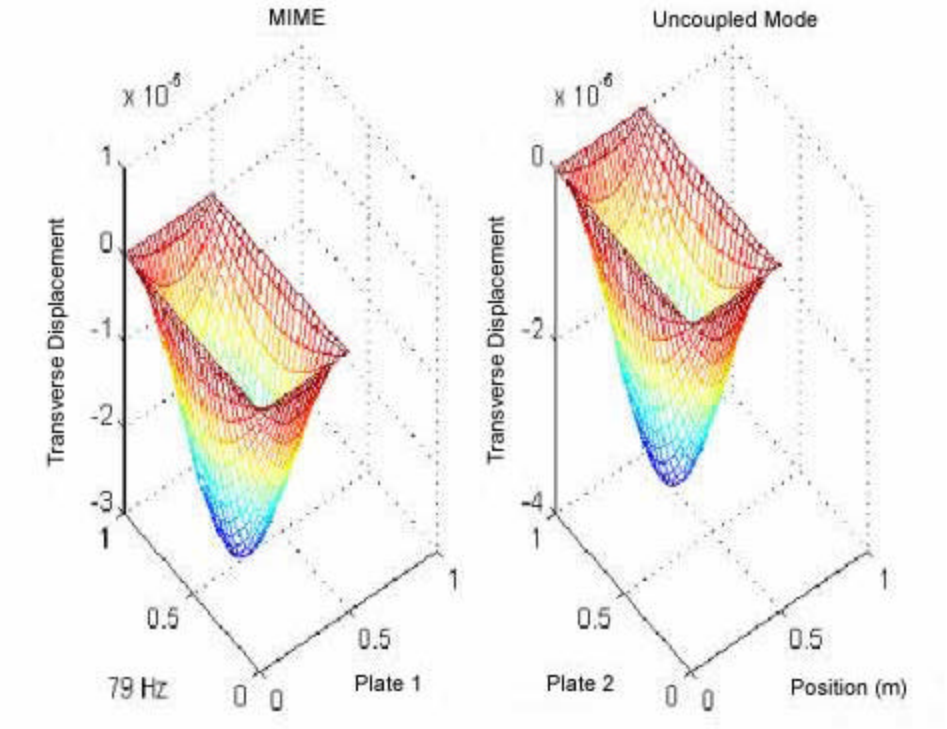

Figure 9 - Transverse displacements associated with the Plates 1 and 2, MIME, 1 st uncoupled mode.

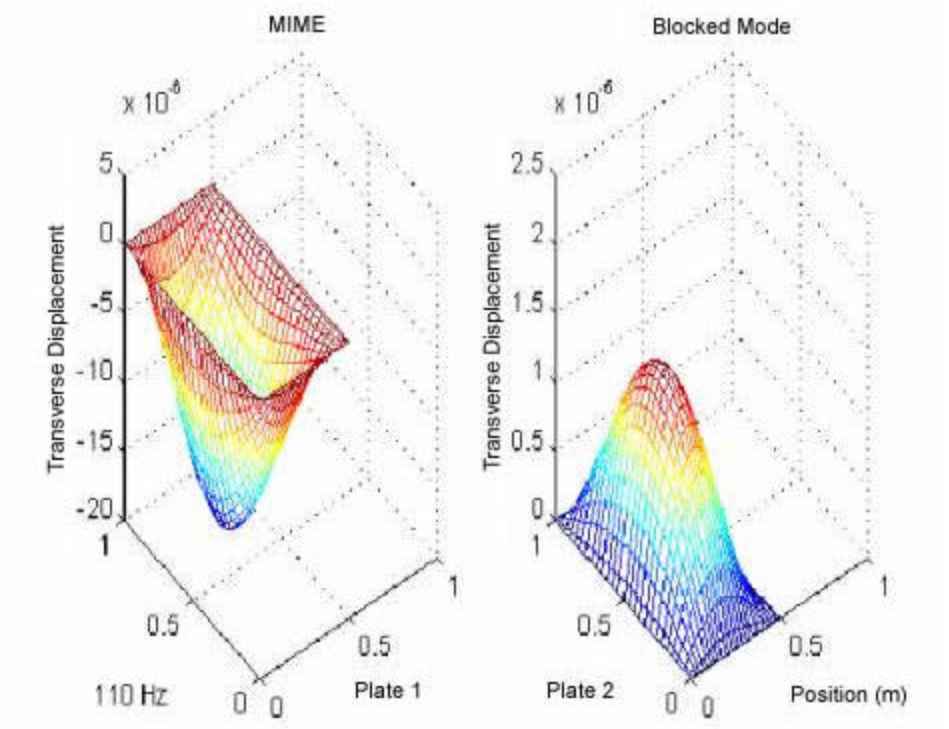

Figure 10 - Transverse displacements associated with the Plates 1 and 2, MIME, 1 st blocked mode.

In Fig. (11) results for P_M distributed along the union line for 79 Hz (left side) and 110 Hz (right side) are compared, as well as the non normalised mistakes between the Cuschieri solution (1996) and MIME.

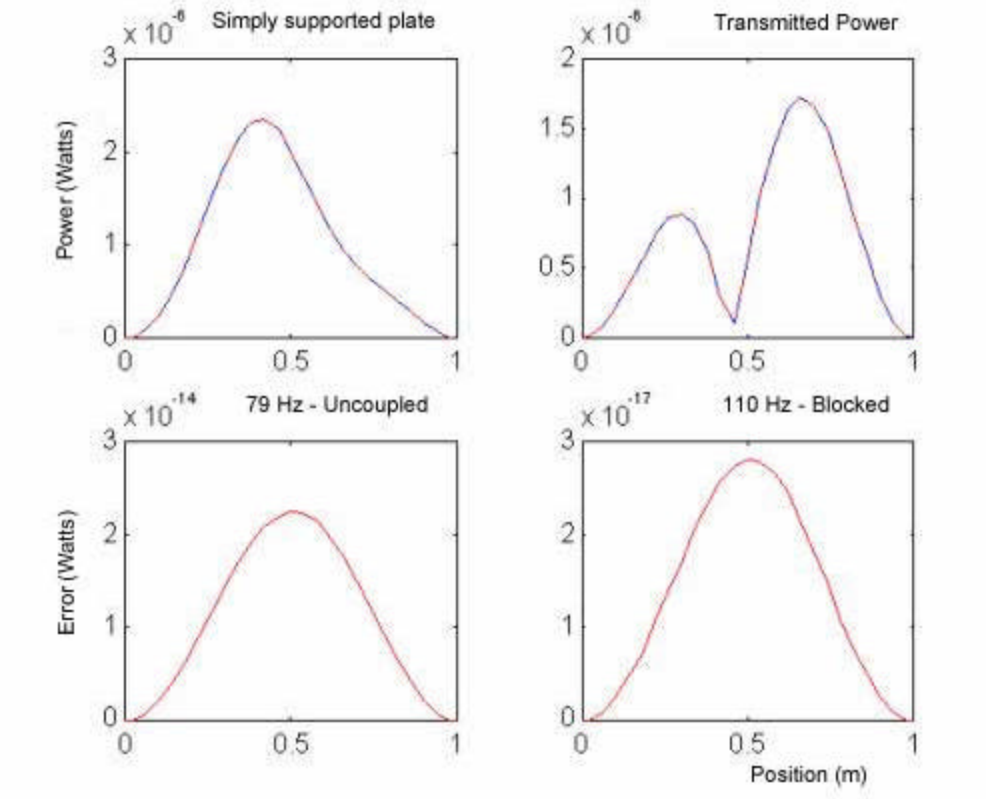

Figure 11 - Power flow along the joint for the 1st uncoupled mode and the 1st blocked mode. a) Analytical method: blue; B) MIME: red.

In Fig. (12), there are the results obtained in the determination of the total power flow through joining and the input power, according to frequency, in both formulations. The spectral resolution used an increase equal to 1 Hz along the whole range. Results obtained through both formulations seem to visually agree along the whole frequency range. However, differences were verified in certain sub-ranges that did not reach 3 dB.

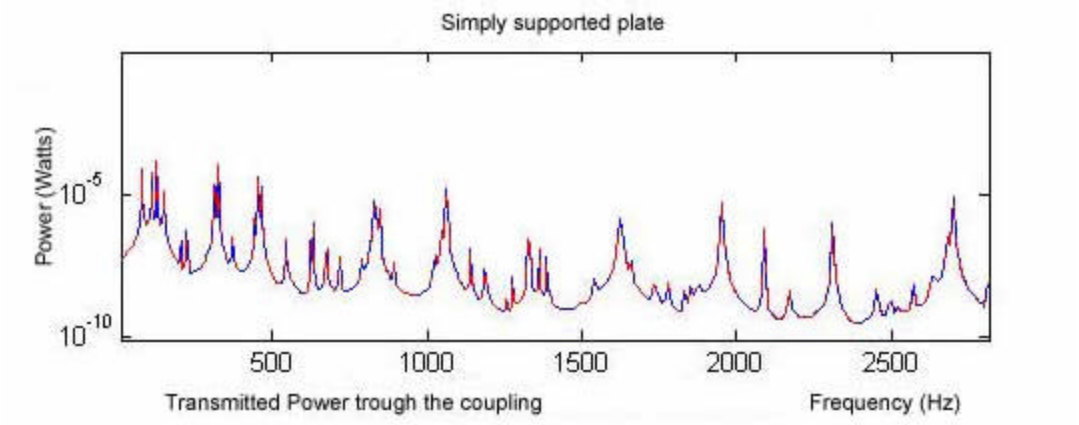

Figure 12 – Power flow along the joint and input power as function of frequency. a) Analytical method: blue; B) MIME: red.

7. Conclusions

MIME showed it is possible to obtain a representation of the response as a displacement, velocity or acceleration, related to a stationary random vibrating field in the frequency domain, as well as for internal forces and power flows along a structural element or transmitted through the coupling of two elements, starting from an experimental methodology of simple execution joined to a mathematical physical device that disregards the most elaborated analytical treatments.

Due to the lack of precision of the tests, results obtained by means of MIME diverged in relation to what has been expected by simulation. The potential of the methodology was verified with the aid of simulations, when it demonstrated it could describe the behavior of magnitudes of interest associated with the vibration movement with good precision, being an efficient alternative to avoid the development of a more complex analytical formulation, as in the determination of the power flow through the joining of two identical plates supported in all sides.

It is intention to extend MIME to the approach of problems that allow a representation of a stationary random sound field associated with the transmission of noise generated by machines, that is irradiated to the surrounding fluid environment through a structure that involves the sources (structure/fluid interaction). More specifically, it is our goal to apply MIME to the analysis of the response of a more complex metallic structure, preferably typically naval, that could be the base of an equipment, and also to check the energy division among the component elements.

8. Bibliography

Gabriel, C. J., *"Proposta de Metodologia para o Estudo da Propagação de Vibrações Aleatórias em Estruturas para Campos Coerentes""*, 2001, Doctorship Thesis, Rio de Janeiro, Universidade Federal do Rio de Janeiro.

Meirovitch, L . ,*"Analytical Methods in Vibrations"*, 1967, London, The Macmillan Company.

Gabriel, C. J.,*"Análise Espectral Parcial – Aplicação ao Estudo de Campos Sonoros"*, 1993, Mastership Thesis, Rio de Janeiro, Universidade Federal do Rio de Janeiro.

Cuschieri, J.M.,*"Parametric Analysis of The Power Flow on an L-shaped Plate Using a Mobility Power Flow Approach"*, 1996, Journal of The Acoustical Society of America, Vol. 91, Pt. 1, May .

Bonifácio, P. R. O., *"Análise do Fluxo de Energia Vibratória Entre Placas Retangulares Simplesmente Apoiadas pelo Método da Mobilidade"*, 1998, Mastership Thesis , Florianópolis, Universidade Federal de Santa Catarina.

Leissa, A . ,*"Vibration of Plates"*, 1993, Columbus, Ohio, The Acoustical Society of America.

Cuschieri, J.M., *"In-Plane and Out-of-Plane Waves Power Transmission Through na L-plate Junction Using The Mobility Power Flow Approach"*, 1996, Journal of The Acoustical Society of America, Vol. 100, Pt.1.

Slama, J. G., *"Sur une Méthode de Decomposition d'um Champ Sonore Aléatoire Stationnaire"*, 1988, Doctorship Thesis, Marseille, Université d'Aix – Marseille II.

Cremer, L. ; Heckl, M. and Ungar, E., *"Structure – Borne Sound"*, 1972, Berlin, Springer – Verlag

Baars, E., *"Fluxo de Potência Vibratória em Componentes Estruturais Tipo Barras e Vigas"*, 1996, Mastership Thesis, Florianópolis, Universidade Federal de Santa Catarina.

9. Copyright Notice

The authors are the only responsible for the printed material included in their paper.

10. Appendix

Tabel (10-1) –Closed solutions for the displacements

$$u_B(x,f) = D_1(f)\cos(\bar{K}_B x) + D_2(f)\,\mathrm{sen}(\bar{K}_B x) + D_3\cosh(\bar{K}_B x) + D_4\,\mathrm{senh}(\bar{K}_B x) \tag{10-1}$$

$$u_L(x,f) = D_5(f)\cos(\bar{K}_L x) + D_6(f)\,\mathrm{sen}(\bar{K}_L x) \tag{10-2}$$

$$q_T(x,f) = D_7(f)\cos(\bar{K}_T x) + D_8(f)\,\mathrm{sen}(\bar{K}_T x) \tag{10-3}$$

$D_i (1 \le i \le 8)$ constants, $\bar{K}_B = K_B(1 - i\eta/4)$, $\bar{K}_L = K_L(1 - i\eta/2)$, $\bar{K}_T = K_T(1 - i\eta/2)$,

Tabel (A-2) – Relationships among displacements, velocities and internal forces

Bending Moment	$M(x,f) = -\bar{E}\,I\,\dfrac{\partial^2 u_T(x,f)}{\partial x^2}$	Longitudinal Force	$A(x,f) = \bar{E}\,A\,\dfrac{\partial u_L(x,f)}{\partial x}$
Shear Force	$Q(x,f) = \bar{E}\,I\,\dfrac{\partial^3 u_T(x,f)}{\partial x^3}$	Torsional Moment	$T(x,f) = \bar{G}\,J_p\,\dfrac{\partial q_T(x,f)}{\partial x}$
Bending Angular Velocity	$w_F(x,f) = i2\pi f\,\dfrac{\partial u_T(x,f)}{\partial x}$	Torsional Angular Velocity	$w_T(x,f) = i2\pi f\,q_T(x,f)$

K_B :bending wave number; k_L : longitudinal wave number; K_T : torcion wave number; E : elasticity modulus;

G : shear modulus; A : area; I : moment of inercia; $\bar{E} = E(1 + i\eta)$ and $\bar{G} = G(1 + i\eta)$

Tabel (A-3) – Equivalence between expressions for closed solution (SF) and MIME

	SF	MIME
Displacement	$u(x,f)$	$\mathrm{Re}\{S_{Fu}(x,f) / (S_{FF}(f))^{1/2}\}$
$P_V(x,f)$	$0{,}5\mathrm{Re}\{Q(x,f)V_B^*(x,f)\}$	$0{,}5\mathrm{Re}\left\{\dfrac{S_{QF}(x,f)S_{F v_B}(x,f)}{S_{FF}(f)}\right\}$
$P_M(x,f)$	$0{,}5\mathrm{Re}\{M(x,f)w_B^*(x,f)\}$	$0{,}5\mathrm{Re}\left\{\dfrac{S_{MF}(x,f)S_{F w_B}(x,f)}{S_{FF}(f)}\right\}$
$P_L(x,f)$	$0{,}5\mathrm{Re}\{A(x,f)V_L^*(x,f)\}$	$0{,}5\mathrm{Re}\left\{\dfrac{S_{AF}(x,f)S_{F v_L}(x,f)}{S_{FF}(f)}\right\}$
$P_T(x,f)$	$0{,}5\mathrm{Re}\{T(x,f)w_T^*(x,f)\}$	$0{,}5\mathrm{Re}\left\{\dfrac{S_{TF}(x,f)S_{F w_T}(x,f)}{S_{FF}(f)}\right\}$

Re : real part of a complex number